Effects of B, C, and Zr on the Structure and Properties of a P/M Nickel Base Superalloy

T. J. GAROSSHEN, T. D. TILLMAN, and G. P. McCARTHY

The boron and carbon levels of a P/M nickel base superalloy were systematically varied in order to determine the mechanisms by which these elements strengthen the alloy, and their optimum concentration. Carbon levels were reduced to 20 ppm while the boron level was varied from 0.02 to 0.10 wt pct. Carbon levels of 0.002 and 0.05 wt pct were also studied, while maintaining a boron concentration of 0.02 wt pct. Zirconium levels were maintained at 0.06 wt pct. The resulting alloys were subjected to identical heat treatments and examined *via* SEM, TEM, and STEM microscopy. The alloys were also subjected to tensile, creep, stress-rupture, and fatigue crack growth tests. Results show that both carbon and boron have a strong influence on the formation of grain boundary precipitates, as expected. Carbon was present as the MC and $M_{23}C_6$ type carbides, while boron combined to form an intergranular M_3B_2 boride. Boron and zirconium were observed to be critical to the alloys' mechanical properties, although boron levels above the solubility limit resulted in no further improvement or debit in strength. Carbon additions resulted in no improvement in properties, indicating the feasibility of a carbon-free P/M superalloy. The role of the minor element additions is discussed in terms of both microstructural features and related strengthening mechanisms.

I. INTRODUCTION

THE importance of minor element additions to the mechanical properties of polycrystalline nickel base superalloys is well established. Certain elements, such as carbon, boron, and zirconium, are reported to significantly improve creep life, rupture strength, and tensile ductility at elevated temperatures.[1,2,3] Carbon additions are reported to form grain boundary precipitates, which when present as discrete particles, are believed to pin grain boundaries and thereby inhibit grain boundary sliding.[4] Boron and zirconium additions are cited for a variety of strengthening mechanisms including (1) decreased grain boundary diffusivity, (2) increased grain boundary interfacial strength, (3) lowering of grain boundary surface energy, (4) removal of tramp elements by precipitating them as stable compounds (*e.g.*, Zr_2S), and (5) by creating changes in fine γ' or $M_{23}C_6$ carbide morphologies.[1,5,7]

Despite the obvious importance of minor element additions, the actual mechanisms by which these elements improve mechanical properties remain unclear. With the advent of P/M processing and the advanced alloy compositions used for gas turbine disk applications, the role of minor element additions and their effect on grain boundary strength becomes increasingly important. This is due to the stringent strength requirements of disk alloys which require fine grain sizes for Hall-Petch strengthening, combined with time dependent mechanical properties such as creep, fatigue crack growth, and stress-rupture strength, which often exhibit intergranular failure modes. Although the advent of single crystal superalloys for turbine blade applications has lessened the impetus for understanding grain boundary structure and chemistry, grain boundaries remain crucial to the strength and performance of P/M nickel base superalloys. Further understanding and optimization of grain boundary chemistry in these alloys is therefore warranted.

The studies reported in this paper compare the properties and structure of a P/M superalloy in which the boron and carbon levels were systematically varied. The roles of the various minor chemistry modifications are discussed in terms of observed microstructural changes and associated strengthening mechanisms.

II. EXPERIMENTAL PROCEDURE

The compositions of the alloys analyzed in this study are listed in Table I. The alloys were prepared from the same master heat with the exception of alloy number 4. Atomization was performed by Homogeneous Metals, Inc., Clayville, New York, and the minor elements were added as late additions to the melt prior to atomization. The powder was processed under inert atmospheres, hot compacted at 1010 °C, and extruded at 1080 °C with a 6:1 extrusion ratio. The alloys were isothermally forged at 1093 °C with a strain rate of 0.25 min^{-1}. All alloys were subjected to the following five-step heat treatment:

1. 1130 °C/2 hrs/oil quench
2. 871 °C/40 min/air cool
3. 982 °C/45 min/air cool
4. 650 °C/24 hrs/air cool
5. 760 °C/4 hrs/air cool

Standard creep, tensile, compact tension, and stress-rupture combination notch/smooth test specimens were machined from the heat treated material. Compact tension specimens were prepared and tested according to the ASTM 399 specification.

Specimens for metallographic examination were prepared from heat treated material using standard practices. STEM/TEM analysis was performed with a Philips 400T microscope with microanalytical X-ray capabilities.

T. J. GAROSSHEN, Research Metallurgist, and G. P. McCARTHY, Electron Microscopist, are with Materials Technology Department, United Technologies Research Center, East Hartford, CT 06108. T. D. TILLMAN is Materials Engineer with Pratt and Whitney Aircraft Company, West Palm Beach, FL.

Manuscript submitted February 19, 1986.

Table I. Analyzed Alloy Compositions* (Nickel Base)

#	B	C	Zr	Co	Cr	Al	Ti	Mo	S†	O†	Pb†	Bi†
1	ND	0.002	ND	18.7	12.5	4.9	4.4	3.3	<10	140	<1	<1
2	0.02	0.003	0.05	18.7	12.4	4.9	4.4	3.2	<10	134	<1	<1
3	0.05	0.002	0.06	18.7	12.5	5.0	4.4	3.3	<10	124	<1	<1
4+	0.10	0.006	0.06	18.8	12.0	5.3	4.4	3.3	<10	180	<1	<1
5	0.02	0.055	0.06	18.3	12.4	5.1	4.4	3.2	<10	92	<1	<1

*wt pct ND = Not Detected (<10 ppm) +1.4 wt pct Nb †ppm

Table II. Tensile Properties of Alloys 1 through 5*

Alloy	Minor Chemistry (Wt Pct)	Test Temperature (°C)	YS (MPa)	UTS (MPa)	EL (Pct)
1	0.002 C	22	1172	1600	25
2	0.02 B, 0.05 Zr, 0.003 C	22	1151	1572	23
3	0.05 B, 0.06 Zr, 0.002 C	22	1138	1565	22
4	0.10 B, 0.06 Zr, 0.006 C	22	1158	1600	20
5	0.02 B, 0.06 Zr, 0.055 C	22	1151	1586	23
1	0.002 C	427	1137	1496	21
2	0.02 B, 0.05 Zr, 0.003 C	427	1103	1489	22
3	0.05 B, 0.06 Zr, 0.002 C	427	1103	1496	23
4	0.10 B, 0.06 Zr, 0.006 C	427	1105	1482	**
5	0.02 B, 0.06 Zr, 0.055 C	427	1123	1537	23
1	0.002 C	704	813	910	4
2	0.02 B, 0.05 Zr, 0.003 C	704	1061	1241	20
3	0.05 B, 0.06 Zr, 0.002 C	704	1041	1227	15
4	0.10 B, 0.06 Zr, 0.006 C	704	1068	1275	**
5	0.02 B, 0.06 Zr, 0.055 C	704	1075	1248	17

*Averages of two tests
**Not measured

Boron and zirconium levels were measured by Inductively Coupled Plasma-Atomic Emission Spectroscopy, whereas carbon levels were measured by the LECO combustion method.

Two noteworthy aspects of the experimental procedures are that the reported chemistries were measured with a reproducible accuracy of better than ±10 pct, and heat treatment temperatures were maintained at ±3 °C. Both of these considerations are important when discussing differences in minor chemistry and associated phase formation.

III. RESULTS

A. *Mechanical Properties*

1. *Tensile results*

The tensile properties of the various alloy modifications are contained in Table II. As shown, the minor chemistry modifications have no apparent effect on room temperature and 427 °C tensile strength or ductility. At room temperature, yield strengths were approximately 1150 MPa, and ultimate tensile strengths were 1565 to 1600 MPa. Tensile elongations were in the 20 to 24 pct range. At 427 °C, the yield strengths dropped to the 1103 to 1137 MPa range and ultimate tensile strengths were approximately 1500 MPa. Tensile elongations remained in the 20 to 24 pct range. Interestingly, at 704 °C the alloy (#1) with no Zr, B, or C additions exhibited a significant decrease in tensile properties. The yield strength of alloy #1 was 813 MPa, whereas alloys 2 through 5 exhibited yield strengths around 1060 MPa. The ultimate tensile strength of alloy #1 also decreased to a value of 910 MPa, whereas alloys 2 through 5 had ultimate tensile strengths between 1241 and 1275 MPa. The tensile elongations of alloy #1 also showed a significant drop at 704 °C to 4 pct, as compared to values of 15 to 20 pct for alloys 2 through 5. In general, alloys 2 through 5 exhibited essentially equivalent tensile properties.

2. *Stress-rupture results*

Stress rupture testing of the various alloy modifications was performed at 732 °C with a uniaxial stress of 655 MPa. Table III summarizes the results and each of the reported values represents the average of two tests. As shown, alloy number 1, which contained no zirconium, boron, and carbon, failed after 6 minutes. In comparison, alloys 2 through

Table III. Stress-Rupture Results for Alloys 1 through 5 (732 °C/655 MPa)

Alloy	Minor Chemistry* Modification	Average Life** (Hours)
1	0.002 C	0.1
2	0.02 B, 0.05 Zr, 0.003 C	69
3	0.05 B, 0.06 Zr, 0.002 C	52
4	0.10 B, 0.06 Zr, 0.006 C	47
5	0.02 B, 0.06 Zr, 0.055 C	67

*Wt pct
**Averages of two tests

5 experienced lives in the range of 47 to 69 hours. Alloy number 5, which contained carbon, failed on average, after 69 hours, whereas alloy number 2 with essentially no carbon and 0.02 wt pct boron failed at 67 hours, indicating that the addition of carbon did not influence the alloy's rupture life. None of the alloys which contained boron and zirconium failed in the notch, although alloy number 1, which contained no zirconium, boron or carbon, did fail in the notch.

3. *Creep results*

The results of creep tests, performed at 704 °C and a stress level of 552 MPa, are shown in Figure 1. Alloy number 1 failed after 54 minutes, whereas the time to 0.2 pct elongation of alloys 2 through 5 were 508, 231, 220, and 348 hours, respectively. Steady state creep rates were similar for alloys 2, 3, and 5 and averaged approximately 4×10^{-4} pct/hr.

4. *Fatigue crack growth tests*

Compact tension specimens were tested in air at 649 °C with a test frequency of 10 cpm and a strain ratio (R) of 0.1. The nominal stress level was 896 MPa. A plot of da/dN *vs* ΔK is found in Figure 2 for alloys 2 through 4. A curve for typical P/M IN-100 is also presented. As shown, 2, 3, and 4 displayed a slight improvement in da/dN at the higher ΔK values. However, at lower ΔK values the crack growth rates were similar for all alloys.

B. *Differential Thermal Analysis (DTA)*

The γ' solvus and incipient melting point of each alloy was measured by DTA, and the resulting values are contained in Table IV. As shown, the addition of boron or carbon had little affect on the γ' solvus. However, the incipient melting point dropped with increasing boron concentration as expected.

C. *Microstructural Analysis*

Microstructural analysis shows a typical trimodal γ' morphology for all alloys after the standard heat treatment as shown in Figure 3. The γ' phase occupies a volume fraction of approximately 65 pct, and the average grain diameter is in the 5 to 10 μm range after heat treatment. A more detailed description of the γ' phase can be found in Reference 6.

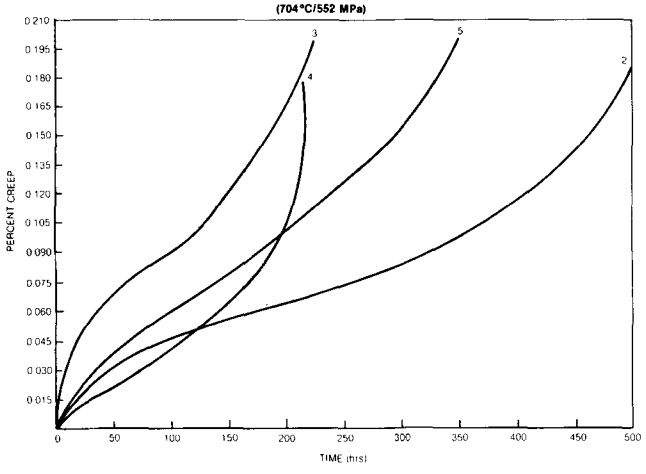

Fig. 1—Creep curves for alloys 2 through 5.

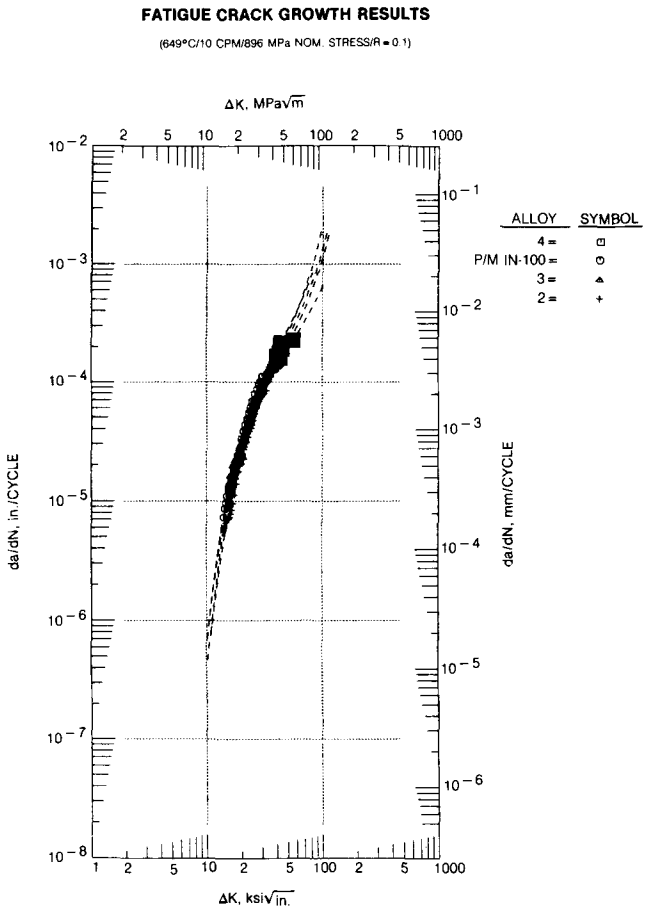

Fig. 2—Plots of ΔK *vs* da/dN for alloys 2 through 5.

Table IV. Differential Thermal Analysis Determinations of γ' Solvus and Incipient Melting Point

Alloy	Incipient Melting Point, °C	γ' Solvus °C	B (Wt Pct)	C (Wt Pct)
1	1282	1197	—	0.002
2	1237	1199	0.02	0.003
3	1231	1198	0.05	0.002
*4	1230	1210	0.10	0.006
5	1247	1196	0.02	0.055

*+1.4 wt pct Nb

TEM micrographs of grain boundaries in the various alloys are contained in Figure 4 and as shown, the alloy with no carbon, boron, or zirconium additions (#1) contained essentially no grain boundary precipitates. In comparison, the alloy which contained boron, carbon, and zirconium (#5) contained appreciable amounts of secondary intragranular and intergranular phases, whereas alloys 2 and 3 contained relatively few grain boundary precipitates. Figure 5 shows the typical structure of alloy 4 which contains 0.10 wt pct of boron. As shown, a relatively large volume fraction of a M_3B_2 boride is present. Figure 5 also contains a typical X-ray spectrum of the boride, and as indicated, it is enriched in molybdenum and chromium. Selected area electron diffraction analysis of a boride precipitate indicates a tetragonal structure with an a_0 of 0.585 nm and a C_0 of 0.315 nm. The minor phase observed in alloys 2 and 3 was also a M_3B_2

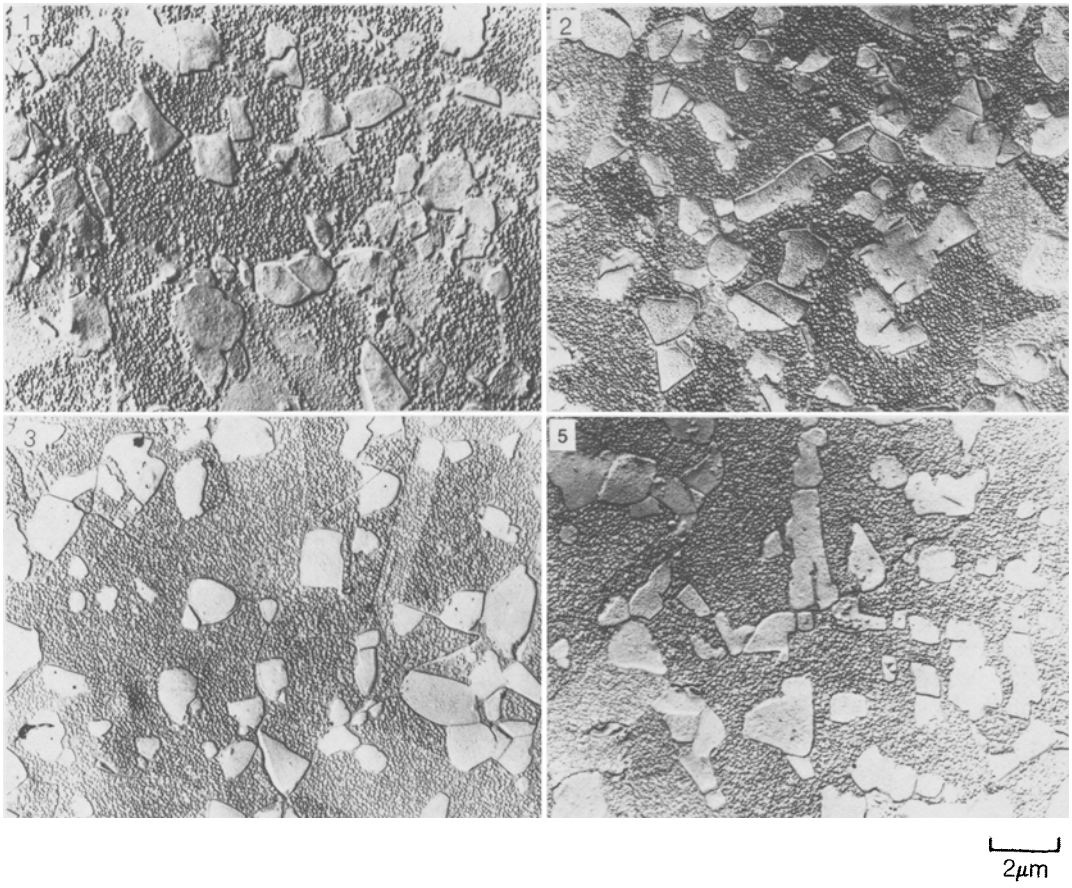

Fig. 3—TEM replicas showing typical γ' structure of alloys 1, 2, 3, and 5 after standard heat treatment.

boride. Alloy 2 contained a very low incidence of the boride, whereas alloy 3 contained a larger amount.

In comparison to alloys 2 through 4, the minor phases observed in alloy 5 consisted primarily of MC and $M_{23}C_6$ carbides, whereas the M_3B_2 boride phase was rarely observed. Examples of the carbide phases and their representative X-ray spectra are shown in Figure 6. The $M_{23}C_6$ carbide and M_3B_2 boride were observed to reside intergranularly, whereas the titanium enriched monocarbides (MC) were typically found at intragranular locations. The alloys also contained the occasional appearance of oxide particles primarily enriched in aluminum. All secondary phases, including the occasional oxide particles, displayed discrete noncontinuous morphologies.

Alloys 1, 2, 3, and 5 were analyzed for differences in fine γ' morphologies with special attention to the regions adjacent to grain boundaries. Figure 7 contains TEM dark-field images which show typical fine γ' areas in each alloy. As shown, no significant differences in fine γ' morphologies were observed for the various minor chemistry modifications.

In general, all alloys showed similar γ' morphologies and grain sizes. The three secondary phases observed were a titanium enriched MC carbide, a $M_{23}C_6$ carbide enriched in chromium and molybdenum, and a M_3B_2 boride enriched in molybdenum and chromium.

IV. DISCUSSION

The results presented in Section III indicate that boron and zirconium are crucial to the alloy's creep and stress-rupture strength and tensile ductility, although boron additions above the solubility limit resulted in no further improvement in strength. In comparison, the addition of carbon (alloy 5) resulted in no additional improvement in mechanical properties.

The roles by which these minor elements strengthen the alloy can be discussed in terms of segregation and precipitation. By segregation, we mean a higher than bulk concentration of an element associated with an interface or crystal defect; whereas, precipitation involves the formation of a distinct phase with its own physical and chemical properties.

A. *Carbon Additions*

In nickel base superalloys, carbon additions generally result in the formation of precipitates such as the MC, M_6C, M_7C_3, and $M_{23}C_6$ carbides.[8] In some alloys sulfocarbides have also been observed.[8] Although the solubility of carbon in nickel is appreciable,[9] the presence of stable carbide forming elements, such as titanium and chromium, leaves little carbon in solution. The method by which carbon strengthens a nickel base superalloy is therefore believed to involve the formation of intergranular carbide precipitates

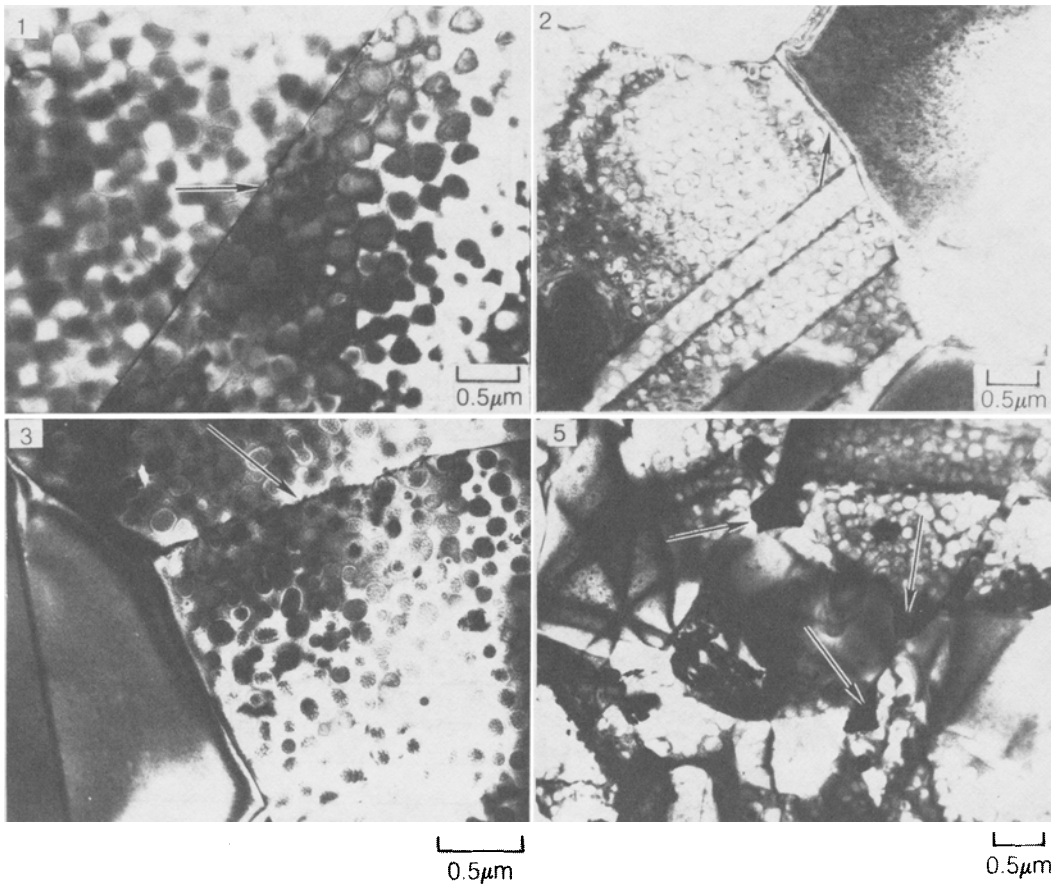

Fig. 4—TEM micrographs showing typical grain boundary phase morphology in alloys 1, 2, 3, and 5 after standard heat treatment.

SEM BACK SCATTERED ELECTRON IMAGE SHOWING BORIDE DISTRIBUTION

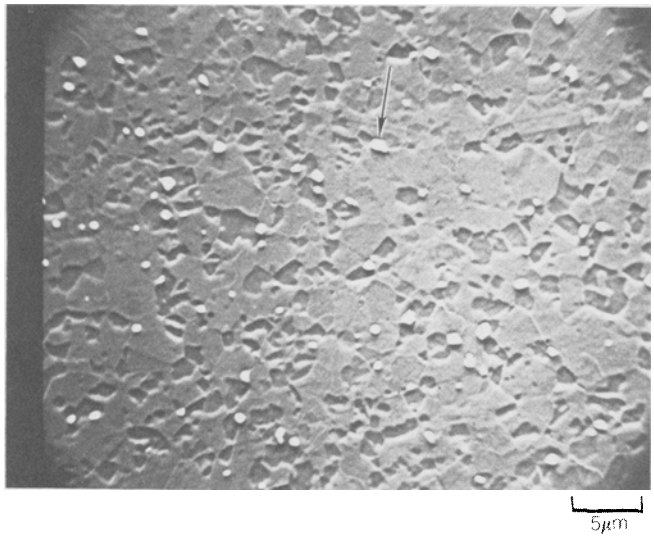

TEM MICROGRAPH AND X-RAY SPECTRA OF INDICATED BORIDE PRECIPITATE

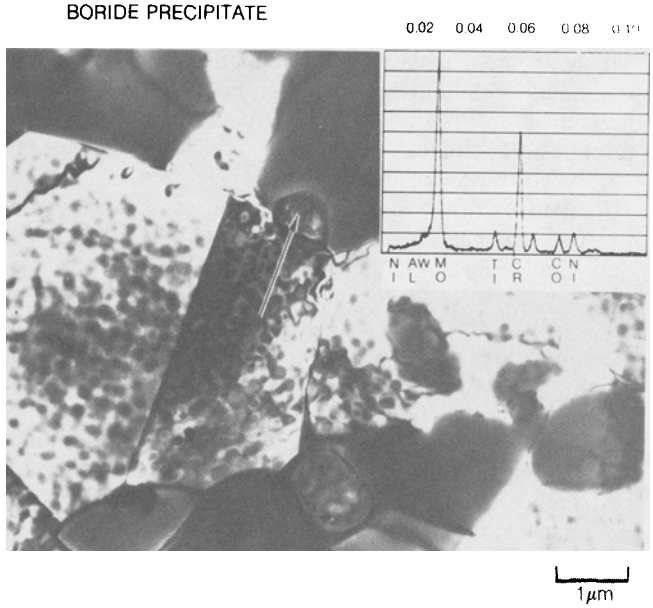

Fig. 5—Microstructure of alloy 4.

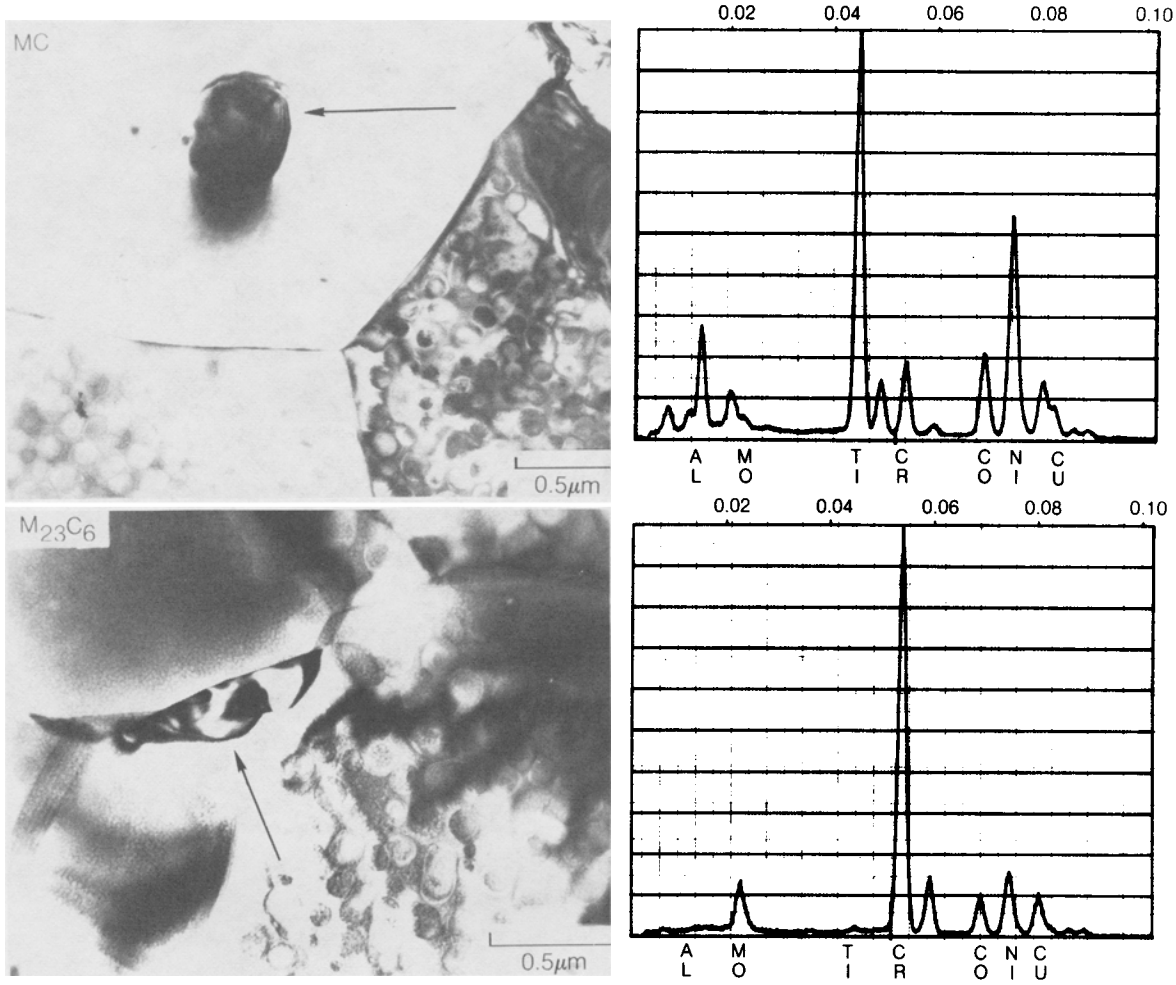

Fig. 6—TEM micrographs and associated X-ray spectra of MC and $M_{23}C_6$ carbides in alloy #5.

which pin grain boundaries and thereby inhibit grain boundary sliding.[10] This strengthening mechanism is expected to be more apparent at elevated temperatures (>0.5 T_m) where grain boundary sliding becomes significant.[11] Carbides may also act as an "unstrengthening" mechanism if they are present as a continuous morphology which creates an easy path for crack propagation.

Comparison of the mechanical properties of the alloys in this study indicates that the carbon addition/carbides are not a significant strengthening factor at the temperatures presently of interest for gas turbine disk applications (RT — 732 °C). Reports of poor rupture properties in nickel base superalloys with low carbon levels may be the result of the improper stabilization of carbides during heat treatment, which results in carbide films at the grain boundaries,[6] or due to higher temperature applications where grain boundary sliding is a predominate deformation mechanism.

At higher temperatures the benefits of grain boundary precipitates are expected to become more apparent. To determine if this was true for this alloy, alloys number 2 and 5 were creep tested at 982 and 871 °C with uniaxial stress levels of 34.47 and 68.95 MPa, respectively. In order to avoid superplastic behavior, the material was heat treated at 1195 °C for two hours to enlarge the grain size, and then subjected to the 5 step heat treatment previously described. After heat treatment the material exhibited an average grain diameter of 75 microns.

The resulting creep curves are presented in Figure 8 and as shown, the alloy (#2) with no carbon addition, and therefore no significant carbide presence, exhibited greater creep rates and shorter times to failure. Although these results indicate that the carbon addition was not crucial to this alloy's strength for the conditions tested, carbon may play other important roles, such as acting as a deoxidizer during melting.[12] The reported oxygen values in Table I support this possibility.

B. *Boron and Zirconium Additions*

The boron levels studied in this investigation involved concentrations of 0.002, 0.02, 0.05, and 0.10 wt pct, while zirconium levels were held at 0.06 wt pct. Since both elements were added simultaneously, they will be discussed jointly.

Historically, boron has been added at very low levels for a variety of reasons including its effect of lowering the alloy's solidus temperature. The role by which boron strengthens a superalloy is believed to involve its segregation to the grain boundaries. This segregation of boron is believed to have one or more of the following effects: (1) increased

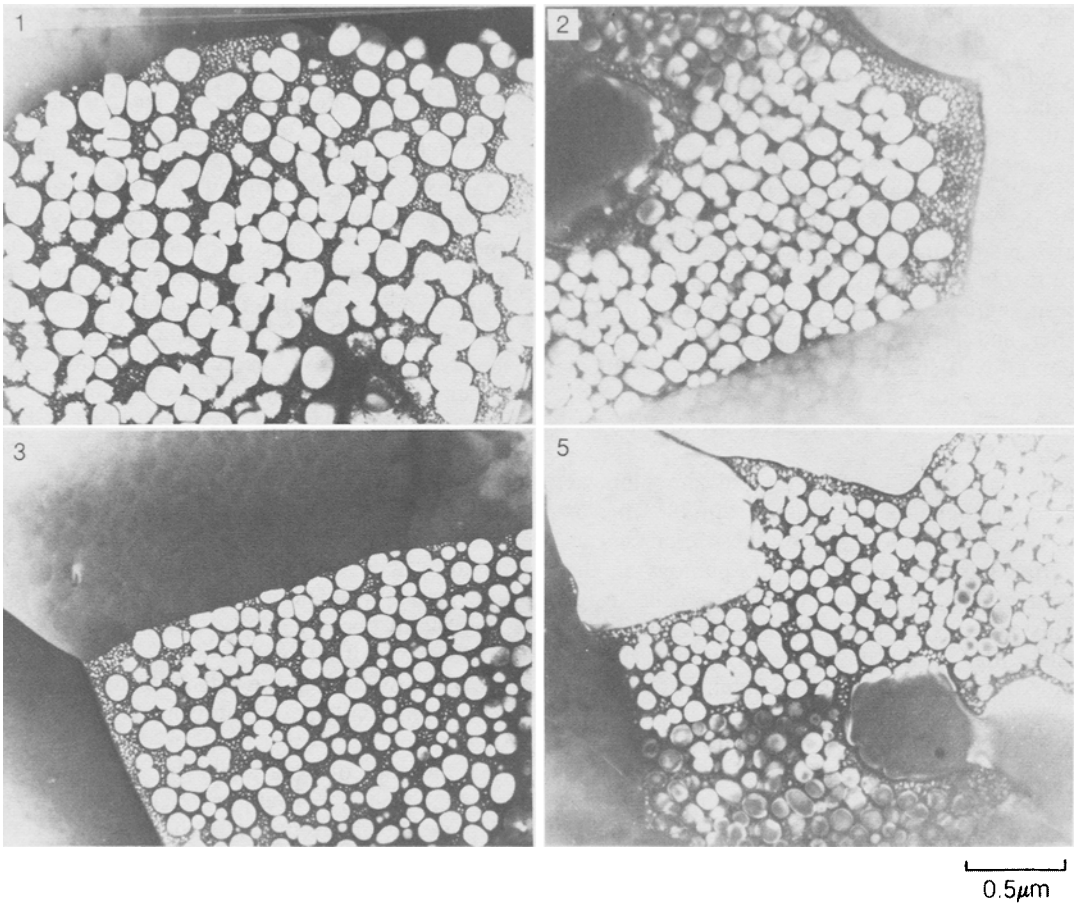

Fig. 7—TEM micrographs from thin foil specimens showing fine γ' morphologies in alloys 1, 2, 3, and 5.

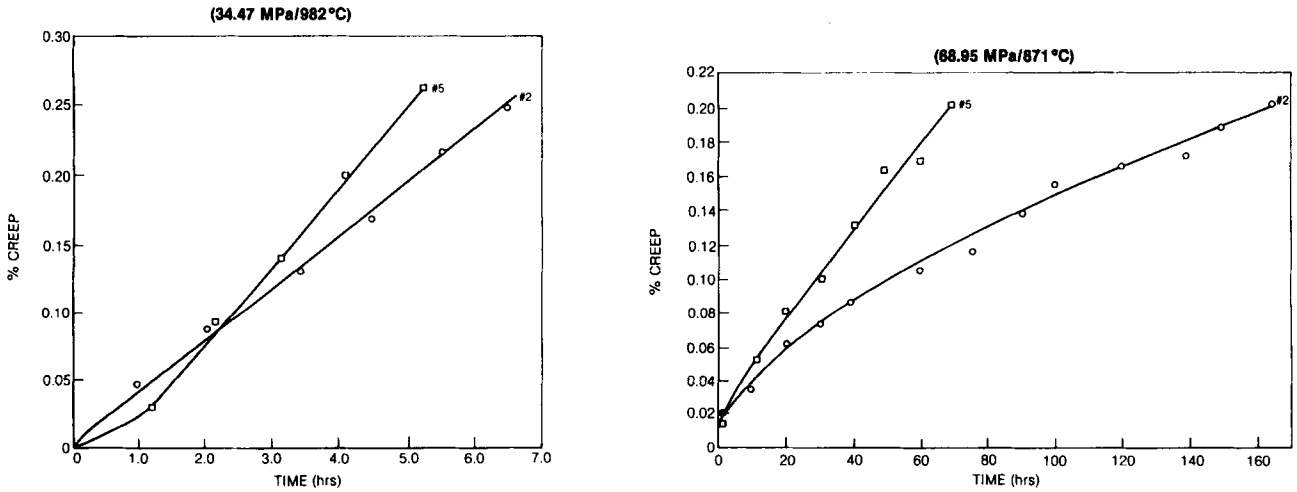

Fig. 8—Creep curves for alloys 2 and 5.

grain boundary cohesion, (2) reductions in grain boundary surface energy, (3) lower grain boundary diffusion rates, and (4) changes in γ' and/or $M_{23}C_6$ morphologies.[13,14,15] Zirconium additions are also cited for similar effects, and the ability to tie sulfur up in an innocuous manner.[16]

When the solubility limit of boron was exceeded in the alloys (3 and 4) studied in this investigation, the presence of boride precipitates was not observed to improve mechanical properties. It is therefore concluded that as a strengthening constituent, boron is important as a segregate, not as a precipitate.

In order to provide an estimate of how much boron is needed for grain boundary segregation in an alloy, the amount of boron necessary to form a monolayer at the grain boundaries was calculated by making the following assumptions: (1) boron has *very* little solubility in the γ or γ' phase, (2) the grains are a stacked structure of dodecatetrahedons, and (3) the atomic spacing of atoms at the grain

boundary is approximately 0.35 nm (similar to the matrix). We also assume that the grain boundaries are the primary sites for segregation. Figure 9 contains a plot of grain size *vs* the calculated boron concentration necessary to form a monolayer at the grain boundaries. As shown, based upon the above assumptions, very low levels of boron are necessary even for the small grain sizes of the material under study. Two of the assumptions, however, are not exactly true. The matrix and γ' phase will have some solubility for boron, and a monolayer is probably larger than the actual degree of boron segregation. However, these two factors offset each other, and the actual amount of boron necessary to strengthen an alloy is still very low. A similar argument applies to zirconium additions with the additional consideration of how much sulfur is present to react with zirconium to form Zr_2S.

Further insight into the role of boron and zirconium as strengthening agents can be obtained from the microstructural analysis. The importance of these elements as "agents" affecting the alloy's fine γ' morphology in the regions adjacent to a grain boundary appears to be insignificant for this alloy. As shown in Figure 7, all alloys exhibited similar fine γ' morphologies. This observation was also true for alloy number 1, which contained no boron, carbon, or zirconium additions.

A similar argument applies to the significance of boron/zirconium additions on the morphology of the $M_{23}C_6$ carbide. Since the alloys without carbon additions showed similar mechanical properties to the alloy with carbon, it appears that the role of these elements with regard to the morphology or coarsening rate of the $M_{23}C_6$ carbide is unimportant for the conditions studied.

Analysis of the elevated temperature tensile results provides further information on the strengthening role of boron and zirconium. As shown in Table II, the alloy which contains no boron, zirconium, or carbon (#1) exhibited significantly lower tensile properties. Due to the abnormality of this result, the test was repeated three times with reproducible results. The lower tensile properties in the absence of grain boundary strengthening elements suggest that the lower strength is related to grain boundary strength at 704 °C. Microstructural analysis supports this idea by showing evidence of intergranular microcracks associated with the 704 °C tensile failures in alloy #1. Due to the relatively rapid strain rates of a tensile test, it would appear that the strengthening role of boron (and possibly zirconium) is at least partially related to grain boundary cohesion. This conclusion is based upon the assumption that diffusion controlled deformation processes are negligible at the strain rates of a standard tensile test.

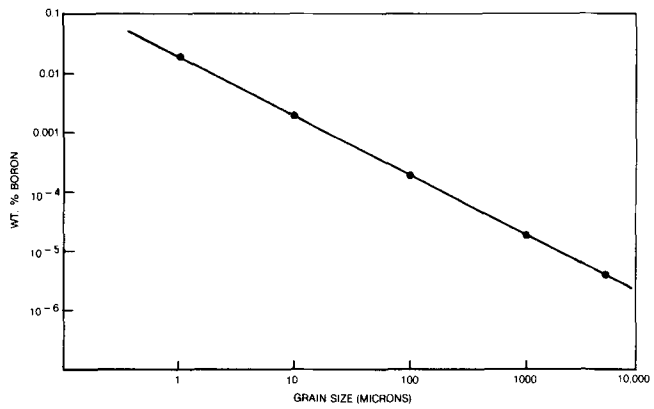

Fig. 9—Grain size *vs* calculated wt pct of boron needed to form a monolayer of boron at the grain boundaries.

Although boron and zirconium were added together, and therefore discussed jointly, it is generally accepted that their effects on grain boundary strength are due to different mechanisms. Evidence of this synergistic effect includes observations of further improvements in creep strength when both elements are added to an alloy as compared to when only one is added.[1] The influence of zirconium is primarily believed to involve the removal of sulfur from the grain boundaries and the lowering of grain boundary diffusion rates. Boron additions are primarily cited for improving grain boundary cohesion, and the results presented support this mechanism.

Experiments to clarify further the role of zirconium would involve comparing the effect of zirconium on the strength of an alloy with *very* low sulfur levels, and measuring Coble creep rates with and without zirconium. Further insight into the role of boron could be achieved in the present alloy in the absence of zirconium.

When discussing the effects of the various minor chemistry modifications, it is informative to compare the role of the minor chemistry addition to the predominant deformation mode of a particular mechanical test. SEM analysis of cross sections of fatigue crack growth, creep, and stress-rupture specimens indicated that these test specimens fail by the formation of creep cavities and intergranular microcracks. The presence of elements such as boron and zirconium, which segregate to and strengthen grain boundaries, can explain the large increase in strength for these test modes. Also, the ultimate tensile strength and ductility of an alloy involve plastic deformation, and at elevated temperatures grain boundaries may act as "weak links" limiting plastic flow. This consideration may explain the relatively low tensile properties of alloy #1 at 704 °C.

In summary, based upon the mechanical properties and microstructural observations discussed, boron levels should be at or below the solubility level, since the appearance of boride precipitates did not improve properties. Carbon additions were observed to have no significant effect on the alloys' strength for the conditions tested, and may therefore not be required for P/M superalloys operating at intermediate temperatures. The absence of carbon in P/M alloys may have beneficial effects on prior particle boundary decoration, fatigue crack initiation at carbide particles, and also eliminate detrimental carbide morphologies.

V. CONCLUSIONS

Based upon the test results and microstructural observations presented, the following conclusions are made:

1. Carbon additions (0.05 wt pct) resulted in no increase in the alloy's strength.
2. Boron and zirconium additions were observed to be very important to the alloy's 704 °C tensile strength and ductility, creep life, and rupture strength.

3. Boron additions above the solubility limit resulted in the intergranular precipitation of a M_3B_2 boride and caused no further improvement in mechanical properties.
4. The addition of zirconium, boron, and carbon had no significant effect on the alloy's γ' morphology.
5. The strengthening role of boron and zirconium was not observed to be related to the $M_{23}C_6$ phase morphology or the fine γ' morphology.
6. The strengthening role of boron was also not observed to be related to the formation of boride precipitates.

REFERENCES

1. R. T. Holt and W. Wallace: *International Metals Review*, March 1976, p. 1.
2. R. F. Decker: in *Source Book on Materials for Elevated Temperature Applications*, ASM Publication, Metals Park, OH, E. F. Bradley, ed., 1979, pp. 275-98.
3. G. P. Sabol and R. Stickler: *Phys. Stat. Sol.*, 1969, vol. 35, p. 11.
4. F. T. Furillo, J. M. Davidson, and J. K. Tien: *Materials Science and Engineering*, 1979, vol. 39, pp. 267-73.
5. A. K. Jena: *Journal of Materials Science*, 1984, vol. 19, pp. 3121-39.
6. T. J. Garosshen and G. P. McCarthy: *Metall. Trans. A*, 1985, vol. 16A, p. 1213.
7. R. M. Brick, R. B. Gordon, and A. Phillips: *Structure and Properties of Alloys*, McGraw-Hill Book Co., New York, NY, 1965, p. 2108.
8. E. P. Whelan and M. S. Grzedzielski: *Metals Technology*, April 1974, p. 186.
9. M. Hansen: *Constitution of Binary Alloys*, 2nd ed., McGraw-Hill Book Co., New York, NY, 1958, p. 374.
10. C. T. Sims: *Journal of Metals*, October 1966, p. 1119.
11. B. Harris and A. R. Bonsell: *Structure and Properties of Engineering Materials*, Longman, New York, NY, 1977, p. 296.
12. J. H. Schneibel and G. F. Peterson: *Scripta Met.*, 1983, vol. 17, p. 353.
13. C. L. White, J. H. Schneibel, and R. A. Padgett: *Metall. Trans. A*, 1983, vol. 14A, p. 595.
14. M. McLean and A. Strang: *Metals Technology*, Oct. 1984, vol. 14, p. 454.
15. M. Burke, J. Greggi, Jr., and G. A. Whitlow: *Scripta Met.*, 1984, vol. 18, p. 91.
16. V. Franzoni, F. Marchetti, and S. Sturlese: *Scripta Met.*, 1985, vol. 19, p. 511.